

Anomalous spectral weight transfer in the nematic state of iron-selenide superconductor

C Cai(蔡淙), T T Han(韩婷婷), Z G Wang(王政国), L Chen(陈磊), Y D Wang(王宇迪), Z M Xin(信子鸣), M W Ma(马明伟), Yuan Li(李源), Y Zhang(张焱)

Citation: Chin. Phys. B . 2020, 29(7): 077401 . **doi:** 10.1088/1674-1056/ab90ec
Journal homepage: http://cpb.iphy.ac.cn; http://iopscience.iop.org/cpb

What follows is a list of articles you may be interested in

Particle-hole fluctuations and possible superconductivity in doped α-$RuCl_3$

Bin-Bin Wang(王斌斌), Wei Wang(王巍), Shun-Li Yu(于顺利), Jian-Xin Li(李建新)

Chin. Phys. B . 2019, 28(5): 057402 . **doi:** 10.1088/1674-1056/28/5/057402

Quantum critical duality in two-dimensional Dirac semimetals

Jiang Zhou(周江), Ya-Jie Wu(吴亚杰), Su-Peng Kou(寇谖鹏)

Chin. Phys. B . 2019, 28(1): 017402 . **doi:** 10.1088/1674-1056/28/1/017402

0-π transition induced by the barrier strength in spin superconductor Josephson junctions

Wen Zeng(曾文), Rui Shen(沈瑞)

Chin. Phys. B . 2018, 27(9): 097401 . **doi:** 10.1088/1674-1056/27/9/097401

Synthesis of large FeSe superconductor crystals via ion release/introduction and property characterization

Dongna Yuan(苑冬娜), Yulong Huang(黄裕龙), Shunli Ni(倪顺利), Huaxue Zhou(周花雪), Yiyuan Mao(毛义元), Wei Hu(胡卫), Jie Yuan(袁洁), Kui Jin(金魁), Guangming Zhang(张广铭), Xiaoli Dong(董晓莉), Fang Zhou(周放)

Chin. Phys. B . 2016, 25(7): 077404 . **doi:** 10.1088/1674-1056/25/7/077404

Interplay of iron and rare-earth magnetic order in rare-earth iron pnictide superconductors under magnetic field

Lei-Lei Yang(杨雷雷), Da-Yong Liu(刘大勇), Dong-Meng Chen(陈东猛), Liang-Jian Zou(邹良剑)

Chin. Phys. B . 2016, 25(2): 027401 . **doi:** 10.1088/1674-1056/25/2/027401

Anomalous magnetoresistance in detwinned $EuFe_2As_2$*

Zhuang Xu(徐状)†, Junxiang Pan(潘俊香)†, Zhen Tao(陶镇), Ruixian Liu(刘瑞鲜), and Guotai Tan(谈国太)‡

Center for Advanced Quantum Studies and Department of Physics, Beijing Normal University, Beijing 100875, *China*

(Received 24 April 2020; revised manuscript received 1 May 2020; accepted manuscript online 7 May 2020)

The in-plane magnetotransport of detwinned $EuFe_2As_2$ single crystal has been investigated. In the antiferromagnetic phase of Eu^{2+} spins, very different magnetoresistance results are observed upon the change of the external magnetic field direction and the current direction. This could be attributed to the tunable orientation of the Eu^{2+} spins under magnetic field. Electron scattering by spin fluctuation, superzone boundary effect, and cyclotron motion of charge carriers are used to interpret the observed anomalous magnetoresistance which is measured by using a current along *a* direction. The remarkable features of magnetoresistance suggest that itinerant electrons strongly couple with the spin configuration of Eu^{2+}, which has a huge influence on the transport properties of $EuFe_2As_2$.

Keywords: magnetoresistance, spin, reorientation, iron pnictides

PACS: 75.47.−m, 74.25.−q, 73.43.Qt **DOI:** 10.1088/1674-1056/ab90e4

1. Introduction

The in-plane electronic anisotropy or electronic nematicity in iron-based superconductors (FeSCs) has triggered tremendous research interest because of their physical properties and possible connection to the microscopic mechanism of high-T_c superconductors.[1–10] It largely surpasses the orthorhombic lattice distortion and has unexpected effect on the electronic properties of FeSCs, similarly in copper-oxide high-T_c superconductors.[11] The tetragonal-to-orthorhombic structural transition associated with the nematic order transition would be expected to broke the C_4 rotation symmetry and result in the in-plane anisotropy of resistivity.[12] However, due to the formation of twin domains below the structural transition, the intrinsic electronic anisotropy is usually obscured for transport measurements in as-grown samples. To explore the nematicity correctly, we must first detwin the sample by applying uniaxial pressure or strong magnetic field to achieve a real orthorhombic state.[13–15]

$EuFe_2As_2$ is a peculiar parent compound of iron pnictides. In addition to the colinear antiferromagnetic order in the FeAs layers with $T_N \approx 188$ K, it exhibits an A-type antiferromagnetic structure of the Eu^{2+} local moments when further cooling down to low temperatures below $T_{Eu} \approx 19$ K (Fig. 4).[16–18] Bulk superconductivity up to about 30 K can be induced by hydrostatic pressure,[19] isovalent substitutions,[20,21] and charge carriers dopings.[22–24] Previous study revealed that magnetic fields within 1 T can fully detwin $EuFe_2As_2$ single crystal, much smaller than that for $BaFe_2As_2$.[15,25] This could be attributed to the biquadratic coupling between Fe^{2+} and Eu^{2+} spins.[26] Below T_{Eu}, a small magnetic field either along *a* or *b* direction can detwin the $EuFe_2As_2$ sample, while above T_{Eu}, only a field parallel to *a* direction can detwin this compound.[15] In addition, the magnetic field could induce a metamagnetic transition with the Eu^{2+} local moments evolved from antiferromagnetic (AFM) to ferromagnetic (FM) order.[15,25,27] Therefore, Eu based iron pnictides offer a unique platform to investigate the interplay of unconventional electronic properties, lattice, and local magnetism.

In fact, the unique AFM order of the $EuFe_2As_2$ system favors a large in-plane electronic anisotropy, especially below T_{Eu}.[6,13,28] Such property is very sensitive to magnetic field and thus can be easily tuned by the field strength and direction, which would be helpful to understand the relationship between magnetism and superconductivity in iron pnictides. Magnetoresistance (MR) is a very useful probe to investigate this issue by directly response to the coupling between itinerant electrons and local moments in magnetic materials.[27,29,30]

Here, we report the in-plane magnetotransport results of $EuFe_2As_2$ single crystal which is fully detwinned by using uniaxial pressure. The MR behaviors simply follow the realignment of the Eu^{2+} spins when increasing the magnetic field along different crystallographic directions. Specifically, MR shows step-like behaviors as the spin configuration of Eu^{2+} is suddenly changed from AFM order to FM order by increasing the external magnetic field along *a* direction. Whereas, MR changes gradually as the spins of Eu^{2+} evolve gradually from AFM order to FM order with increasing external magnetic field along *b* or *c* direction. More interestingly, the sign of MR seems to be locked by the current direction below T_{Eu} under in-plane magnetic field, it is always negative when the current is parallel to *a* direction ($I \parallel a$) but almost positive when $I \parallel b$, which closely resembles to the anisotropic MR in $La_{0.7}Sr_{0.3}MnO_3$ films.[31] Our results give clear evidence of the coupling between itinerant electrons and the local moments of Eu^{2+} in $EuFe_2As_2$, and thus provide a new way to

*Project supported by the Fundamental Research Funds for the Central Universities, China (Grant No. 2014JJCB27).

†These authors contributed equally.

‡Corresponding author. E-mail: tangt@bnu.edu.cn

© 2020 Chinese Physical Society and IOP Publishing Ltd

tune the in-plane anisotropy as well as the electronic nematicity in FeSCs.

2. Experimental details

The single crystals of $EuFe_2As_2$ were grown by the self-flux method.[21,27] The orientations of the crystals were determined by the x-ray Laue method and the samples were cut into 3.4 mm × 3.0 mm × 0.6 mm thin plates along *ab* direction in orthorhombic configuration. Resistivity measurements were performed on a Quantum Design physical property measurement system (PPMS@DynaCool-14T) at Beijing Normal University by using Montgomery method[32] with high-quality $EuFe_2As_2$ single crystals. Besides, a 4-probe method was also executed on the same samples in order to verify the results of Montgomery method.

3. Results and discussion

The magnetization results on the twinned samples were firstly presented. In Fig. 1(a), we applied a magnetic field within *ab*-plane and measured $M(H)$ loops at different temperatures. Field-induced metamagnetic transition associated with the reorientation of local magnetic moments of Eu^{2+} is clearly observed in the magnetically ordered compounds. For example, the system is in an AFM ground state at 4 K, The magnetization displays a linear dependence on the in-plane magnetic field at low field [inset of Fig. 1(a)]. As the field increases, a partially polarized magnetic (PPM) state of Eu^{2+} arises at 0.6 T. This transition could be clearly observed in $\chi(H) = \mathrm{d}M/\mathrm{d}H$ as a sharp peak which is defined as H_1 [Fig. 1(b)]. The magnetization around H_1 exhibits a small hysteresis with the magnetic field [inset of Fig. 1(a)], implying a first-order transition. In the PPM intermediate state, the susceptibility displays a plateau between H_1 and H_{crit}. Beyond H_{crit}, the system evolves into a fully polarized magnetic state (FPM) or FM state. As the temperature increases above T_{Eu}, both H_1 and H_{crit} disappear which indicates a breakdown of the long-range magnetic order of Eu^{2+}. The *T*–*H* phase diagram is shown in the inset of Fig. 1(b). T_{Curie} is the transition temperature of Eu^{2+} spins from paramagnetic order (PM) to ferromagnetic order. Because of the small magnetic hysteresis, the rapid increase in *M* around H_1 is unlikely due to a spin-flop transition, it is most likely a metamagnetic transition. The small hysteresis in our results is similar to previous magnetization measurement in Ref. [27], but it is unlike that in Ref. [15] in which there is almost no hysteresis in $M(H)$. Irrespective of the small hysteresis, the magnetic field dependent *M* shows an abrupt jump in Ref. [15] which is associate with the spin-flip. As the magnetic field increases, the local moments flip from one easy axis to another equivalent easy axis without subsequent reorientation. Such spin flipping effect has been identified by infrared spectroscopy[15] and neutron scattering experiment[25] in $EuFe_2As_2$. The spin-flip indicates that anisotropic energy is larger than Zeeman energy in this system, even though both of them are responsible for the observed spin–lattice coupling.[25]

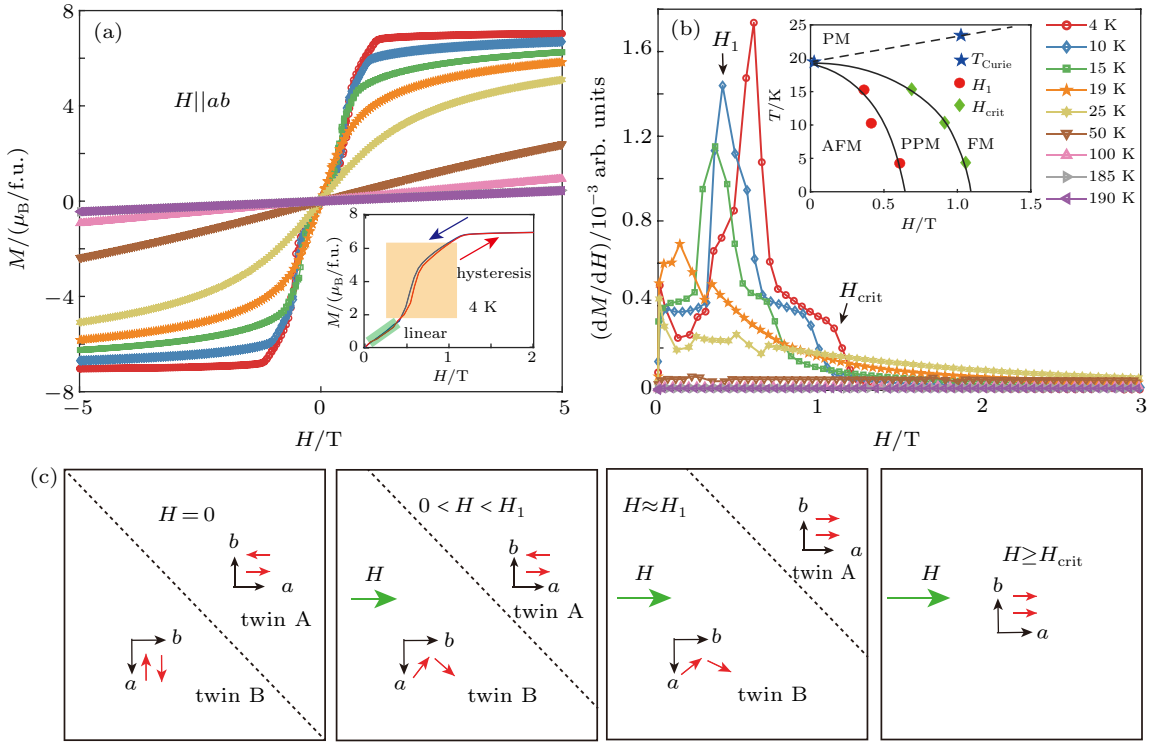


Fig. 1. Magnetization results of twinned $EuFe_2As_2$. Field dependence of magnetization with the *H* parallel to *ab* plane at various temperatures (a) and the corresponding $\mathrm{d}M/\mathrm{d}H$ (b). The expanded $M(H)$ plot at 4 K is shown in the inset of (a). The red and blue arrows represent the measuring setup with increasing field and decreasing field, respectively. Inset of (b) shows the magnetic phase diagram for twinned $EuFe_2As_2$, the data about T_{Curie} gets from the neutron scattering result.[25] (c) Sketch of the magnetic field dependent twin distribution and spin configuration of $EuFe_2As_2$ below T_{Eu}.

As aforementioned the persistent detwinning effect could be induced by external magnetic field in $EuFe_2As_2$. Combining with the previous study,[15] to a certain extent, H_1 and H_{crit} can reflect the spin-flip process and the detwinning process when increasing the magnetic field, as shown in Fig. 1(c). For $H = 0$, the crystal is twinned and the domains are equally distributed, the Eu^{2+} spins are ordered in A-type antiferromagnetism below T_{Eu} with the moments directions along a axis, as shown in the first panel of Fig. 1(c). After applying an external field, twin B with $b \parallel H$ gets energetically favored and then grows. The spins of Eu^{2+} in twin B begin to deviate from their original direction to the direction of the external field, while the spins in twin A are robust and their directions are still maintained. With a further increasing magnetic field, the Eu^{2+} spins in twin A flip along the external field direction and the spins in twin B further deviate from their original direction. When the field exceeds H_{crit}, all Eu^{2+} spins are along the external field, and twin A and twin B merge together to a single FM domain. We note that Eu^{2+} is an S-state rare-earth ion possessing $4f^7$ electrons with $M_{sat} = gS = 7.0\ \mu_B$/f.u. for $g = 2$ and the total electron spin $S = 7/2$. M finally saturates to 6.9 μ_B/f.u. above 1.0 T at 4 K in our experiment, which is very close to the theoretical prediction.

Figure 2 shows the in-plane resistivity [Figs. 2(a)–2(c)] and the resistivity anisotropy [Fig. 2(d)] in detwinned $EuFe_2As_2$. The resistivity anisotropy is defined as $\delta = (\rho_b - \rho_a)/(\rho_a + \rho_b)$. Figure 2(a) shows the zero field measurements of in-plane resistivity. Linear temperature dependent ρ_a and ρ_b are found above the structure transition T_s and the AFM transition T_N ($T_s \approx T_N \approx 188$ K). Resistivity anisotropy is clearly visible already at temperatures above T_s [Fig. 2(d)]. This is very similar to the nematic fluctuations observed in other iron pnictides.[1,2,13] As the temperature decreases, an obvious rise of ρ_b around T_s and a rapid decline of ρ_a are observed. As the temperature is lowered further, small kinks appear both in ρ_a and ρ_b at 19 K which are corresponding to the formation of AFM order of the Eu^{2+} spins. Figures 2(b) and 2(c) are the temperature dependent ρ_a and ρ_b with external field applying along b and c directions, respectively, where such kinks vanish due to the full suppression of AFM order of the Eu^{2+} spins when $H = 3$ T. We would like to emphasize that neither pressure nor magnetic field has much impact on T_s and T_N since they remain at 188 K for all measurements. We compare the resistivity anisotropy under different field geometries in Fig. 2(d). The maximum resistivity anisotropy is about 17% around T_s. In the AFM ordered state of iron pnictides, the resistivity anisotropy is only approximately associated with uniaxial strain and detwinning ratio in the partially twinned state,[32] the resistivity anisotropy of 17% indicates that the sample is well detwinned. All the resistivity anisotropy increases dramatically at T_s and then decreases with temperature decreasing. The resistivity anisotropy in field is only a little smaller than the zero field case below T_s. However, they cross around T_{Eu}, this is likely due to the detwinning effect of the external field in the $EuFe_2As_2$ system.

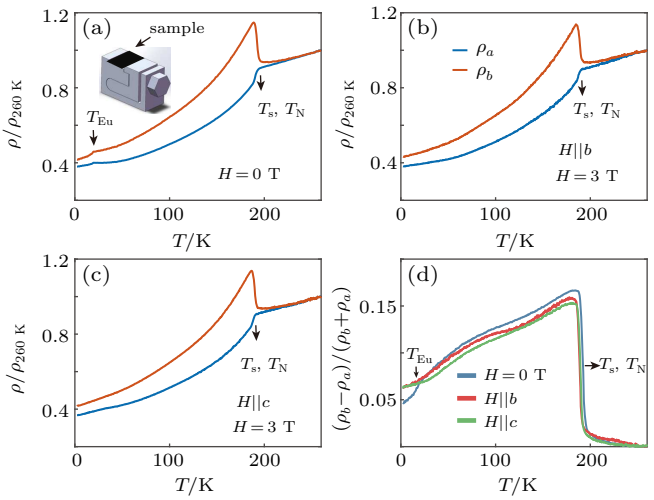


Fig. 2. Resistivity anisotropy of detwinned $EuFe_2As_2$. (a)–(c) Temperature dependence of in-plane resistivity (ρ_a, ρ_b) with no field, the field parallel to b, and the field parallel to c direction, respectively. The resistivity is measured by using Montgomery method. The uniaxial strain cell is shown in the inset of (a). (d) The temperature dependent resistivity anisotropy.

The in-plane MR in the detwinned $EuFe_2As_2$ is illustrated in Fig. 3 which is defined as MR $= (\rho(T,H) - \rho(T,H=0))/\rho(T,H=0)$. Figures 3(a)–3(c) are the MR results with current $I \parallel a$ while the field is parallel to a, b, and c directions, respectively. Figures 3(d)–3(f) are the corresponding MR with current $I \parallel b$. In Fig. 3(a), the MR exhibits different behaviors below and above T_{Eu}. At 4 K, MR increases slightly as the magnetic field increases and reaches a maximum and then it has a step-like decrease with increasing the magnetic field further. The magnitude of MR drops to -4% at $H_{crit} \approx 0.7$ T and then gradually increases with increasing external field. Both the small positive MR at low field and the sudden drops of MR around the critical fields are only observed below T_{Eu}, which indicate that the itinerant electrons are intimately related to the change of ordering of the Eu^{2+} spins in this system as discussed below. The initial positive MR at the low magnetic field could be explained by the theory proposed in Ref. [33], in which a positive MR in the AFM state could be ascribed to that the conduction electrons are scattered by local magnetic moments. The abrupt decrease of MR is associated with the abrupt spin reorientation transition of the Eu^{2+} moments from AFM to FM configuration and could be understood through the superzone boundary effect.[34] This phenomenon has been already found in some other rare-earth transition metal compounds.[35,36]

In the $I \parallel a$ with temperature below T_{Eu} case, the MR with external field along b and c directions [Figs. 3(b) and 3(c)] has two major differences in comparison to the $H \parallel a$ case [Fig. 3(a)]. Firstly, there is not any initial small positive MR

at the low magnetic field. Secondly, around the critical field, the MR does not decrease suddenly but almost decreases linearly as the magnetic field increases. Such differences could be attributed to different Eu^{2+} spins' rearranged models. For the external field parallel to a direction case, the Eu^{2+} spins do not change below the critical field, they only flip suddenly at the critical field and then the spin moments are parallel to the direction of the external field [Figs. 1(c) and 4(a)]. For the external field parallel to b or c direction case, the Eu^{2+} spins start to rotate at the initial external field, and then the Eu^{2+} spins enter a PPM intermediate state. After the field exceeds the threshold value, all Eu^{2+} spins are completely realigned with FM configuration along b or c direction [Figs. 1(c), 4(b), and 4(c)]. Figure 4 shows how the Eu^{2+} spins change with increasing magnetic field of different directions. Once applying the external field along b or c direction, the Eu^{2+} spins are in the PPM state rather than the real AFM order. That is the reason why we did not observe the positive MR at the initial field. With further increasing magnetic field, the MR decreases linearly, which is consistent with that the spins of Eu^{2+} reorientate gradually along the direction of the external field. We note that, above the critical field, the low temperature MR in the FM state starts to increase with increasing magnetic field. This could be explained as follows.[34] The increased magnetic field will suppress the spin fluctuation in a FM system, and thus lead to the decreasing MR. However, if the cyclotron motion of the conduction electron plays a role, it will enhance the MR as the magnetic field increases.[37] The charge carriers scattering time and cyclotron frequency are two critical parameters in determination of the contribution of cyclotron motion to the MR. The carriers scattering time becomes longer at low temperature and the cyclotron frequency increases within increasing external field. Therefore, under low temperature and high magnetic field, the cyclotron motion of charge carriers is the dominating contribution to MR. As a result, the MR increases linearly after the spins of Eu^{2+} enter the FM order. We can get the slope by fitting the linear increase of MR. In Fig. 3(b), the slope decreases as the temperature increases from 4 K (red dashed line) to 10 K (blue dashed line), it is a direct result of cyclotron motion on MR due to the increase of temperature. We also note that the slopes in Figs. 3(a) and 3(c) are smaller than that in Fig. 3(b) even though at the same temperature, that means the cyclotron motion has stronger influence on MR when the magnetic field is along b direction. The slopes vanish at 10 K in Figs. 3(a) and 3(c) within our measurement range, which also supports this argument.

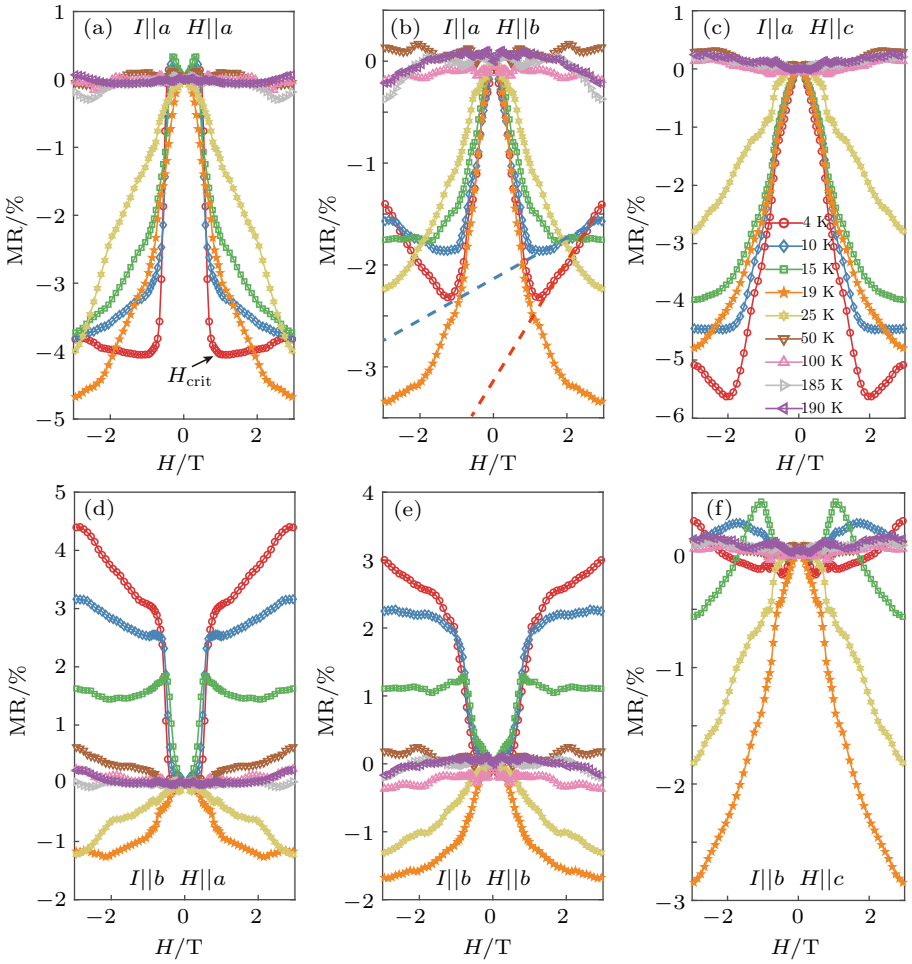


Fig. 3. The in-plane magnetoresistance results of detwinned $EuFe_2As_2$. (a)–(c) The MR results with current $I \parallel a$ while the magnetic field is parallel to a, b and c directions, respectively. (d)–(f) The corresponding MR results with $I \parallel b$.

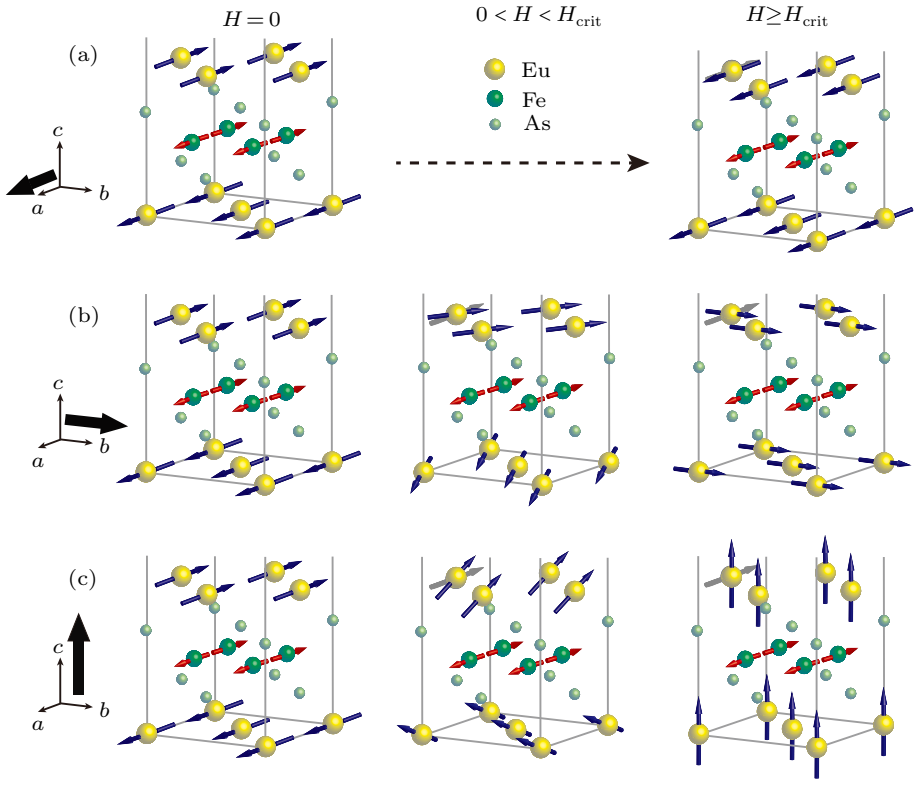


Fig. 4. $EuFe_2As_2$ crystal and magnetic structure (Eu atoms (yellow) and spins (blue), Fe atoms (green) and spins (red), and As atoms (celadon)), and the spin configuration of Eu^{2+} dependent on an external magnetic field along *a* (a), *b* (b), and *c* direction (c), respectively. The black arrows are the applying external magnetic field and the length of the black arrows means the magnitude of the magnetic field. The gray arrows are the original spins of Eu^{2+}.

Next, consider the $I \parallel b$ case [Figs. 3(d)–3(f)]. MR becomes positive below T_{Eu} when applying external field within *ab* plane. This is quite different with that when $I \parallel a$. However, the changing trends of MR show similar behaviors around the critical field no matter what the current direction is. The typical features of MR could be the result of different orientate models of Eu^{2+} spins regardless of the current direction and the applying external field direction. A positive MR is clearly observed once the temperature is higher than T_{Curie} in Fig. 3(d). With applying the external field perpendicular to *ab* plane, the situation becomes much complicated below T_{Eu} [Fig. 3(f)]. If we neglect that, we can also find the common characteristic of all MR. When the temperature is above T_{Eu} and below T_{Curie}, all MR is negative and increases with increasing temperature at 3 T. This is consistent with that the magnitude of the Eu local moments keeps decreasing with increasing temperature in the FM state. The MR effect is not detectable at high temperature due to the oscillation of MR in our experiment.

To verify the availability of data by using the Montgomery method, we also measured MR by using the 4-probe method on the same detwinned samples [Fig. 5(a)]. The result is almost the same as that in Fig. 3(e). Thus, both methods give out the same MR result. We also measured the MR on the twinned $EuFe_2As_2$ [Fig. 5(b)]. The positive MR at the initial magnetic field is larger than that in Fig. 3(a). This could be attributed to the MR in twin B [Fig. 1(a)] in which the magnetic field and current are both parallel to *b* direction, this is most likely the situation in Figs. 3(e) and 5(a). With further increasing magnetic field, twin A is dominant [Fig. 1(c)] and the situation is similar to that in Fig. 3(a). Therefore, the MR in the twinned $EuFe_2As_2$ is almost the average result of the MR in twin A and twin B.

Figure 6 summarizes the magnetic phase diagrams for the detwinned $EuFe_2As_2$. Figures 6(a) and 6(b) correspond to the reorientation models of Eu^{2+} spins for the magnetic field parallel to *a* direction and the magnetic field parallel to *b* and *c* direction, respectively. As shown in Fig. 6, the real AFM state only exists at a narrow range of magnetic field when the field is parallel to *b* or *c* direction, whereas it could insist up to the critical fields when the external field is parallel to *a* direction. Based on the critical field at the same temperature, we can find that *a* is the easy axis for magnetization while *c* is the hard axis for magnetization. Finally, we also note that H_{crit} in magnetization experiment [inset of Fig. 1(b)] locates between the critical field with magnetic field parallel to *a* direction and that with magnetic field parallel to *b* direction in magnetoresistance experiment (Fig. 6), so that it is an average of the two critical fields.

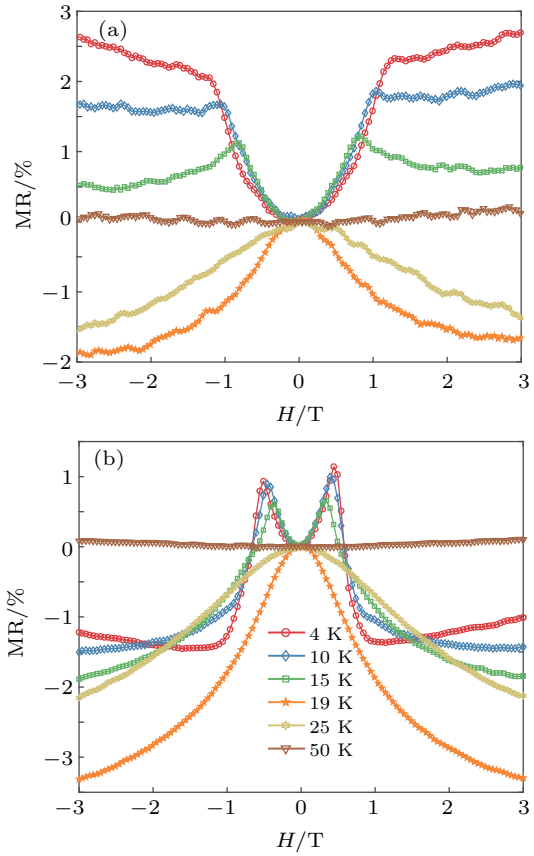


Fig. 5. The MR results by using 4-probe method. (a) The MR results on detwinned $EuFe_2As_2$ with both current and external field parallel to b direction. (b) The MR results with $I \parallel H$ in twinned $EuFe_2As_2$.

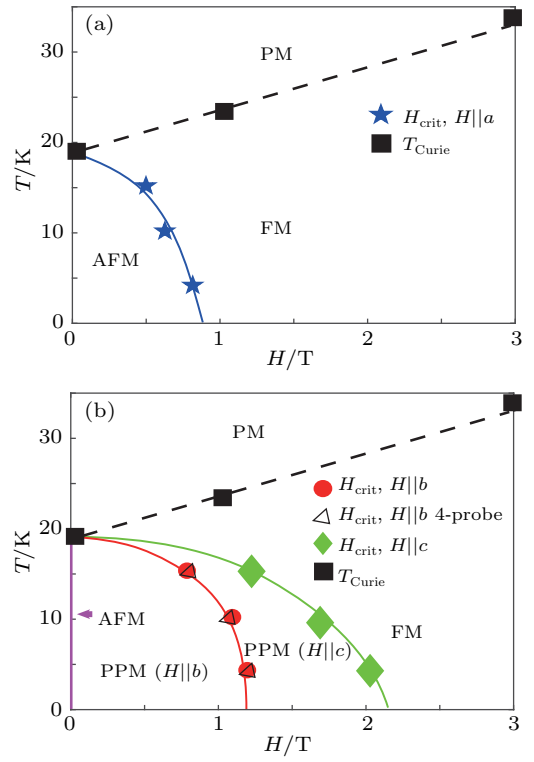


Fig. 6. Magnetic phase diagrams in detwinned $EuFe_2As_2$ with the field parallel to a direction (a) and the field parallel to b or c direction (b). A real AFM state only exists at a narrow range of magnetic field when the magnetic field is parallel to b or c direction (the purple area in (b)). PPM refers to the partially polarized magnetic state.

4. Conclusion

In summary, we study the in-plane resistivity and MR in the detwinned $EuFe_2As_2$. Previous study on the twinning $EuFe_2As_2$ proposed that the changes in MR can be attributed to the magnetic detwinning and electron–spin scattering.[34] In our present MR study without the disturbance of twinning effect, we can conclude that the change of MR follows the configuration of the Eu^{2+} spins, which provides a direct evidence of the coupling between itinerant electrons and spins of Eu^{2+}. Furthermore, within our experiment resolution, we did not observe strong MR when the temperature approaches T_N, this is due to the small ordered moments of Fe^{2+} compared with Eu^{2+}. While the magnitude of MR is dependent on the field geometry, the sign of MR seems to only follow the current directions. Therefore, the charge carriers in $EuFe_2As_2$ appear to have a remarkably strong coupling with the spin order of Eu^{2+}, which plays an important role in determining their transport properties.

Acknowledgment

We thank Pengcheng Dai, Xingye Lu, and Huiqian Luo for helpful discussions.

References

[1] Dai P C 2015 *Rev. Mod. Phys.* **87** 855
[2] Lu X Y, Park J T, Zhang R, Luo H Q, Nevidomskyy A H, Si Q and Dai P C 2014 *Science* **345** 657
[3] Tian L, Liu P P, Xu Z, Li Y, Lu Z, Walker H C, Stuhr U, Tan G T, Lu X Y and Dai P C 2019 *Phys. Rev. B* **100** 134509.
[4] Rosenthal E P, Andrade E F, C. Arguello J, Fernandes R M, Xing L Y, Wang X C, Jin C Q, Millis A J and Pasupathy A N 2014 *Nat. Phys.* **10** 225
[5] Luo H Q, Yamani Z, Chen Y C, Lu X Y, Wang M, Li S L, T. Maier A, Danilkin S, Adroja D T and Dai P C 2012 *Phys. Rev. B* **86** 024508.
[6] Fisher I R, Degiorgi L and Shen Z X 2011 *Rep. Prog. Phys.* **74** 124506
[7] Tanatar M A, Blomberg E C, Kreyssig A, Kim M G, Ni N, Thaler A, Budko S L, Canfield P C, Goldman A I, Mazin I I and Prozorov R 2010 *Phys. Rev. B* **81** 184508
[8] Yi M, Luc D, Chu J H, Analytis J G, Sorini A P, Kemper A F, Moritz B, Mo S K, Moore R G, Hashimoto M, Lee W S, Hussain Z, Devereaux T P, Fisher I R and Shen Z X 2011 *Proc. Natl. Acad. Sci. USA* **108** 6878
[9] Chu J H, Kuo H K, Analytis J G and Fisher I R 2012 *Science* **337** 710
[10] Fernandes R M, Chubukov A V and Schmalian J 2014 *Nat. Phys.* **10** 97
[11] Halbritter J 1993 *Phys. Rev. B* **48** 9735
[12] Avci S, Chmaissem O, Allredl J M, Rosenkranz S, Eremin I, Chubukov A V, Bugaris D E, Chung D Y, Kanatzidis M G, Castellan J P, Schlueter J A, Claus H, Khalyavin D D, Manuel P, Daoud-Aladine A and Osborn R 2014 *Nat. Commun.* **5** 3845
[13] Chu J H, Analytis J G, DeGreve K, McMahon P, Islam Z, Yamamoto Y and Fisher I R 2010 *Science* **329** 824
[14] Blomberg E C, Tanatar M A, Kreyssig A, Ni N, Thaler A, Hu R, Budko S L, Canfield P C, Goldman A I and Prozorov R 2011 *Phys. Rev. B* **83** 134505
[15] Zapf S, Sting C, Post K W, Maiwald J, Bach N, Pietsch I, Neubauer D, Löhle A, Clauss C, Jiang S, Jeevan H S, Basov D N, Gegenwart P and Dressel M 2014 *Phys. Rev. Lett.* **113** 227001
[16] Tegel M, Rotter M, Wei V, Schappacher F M, Pöttgen R and Johrendt D 2008 *J. Phys.: Condens. Matter* **20** 452201
[17] Jeevan H S, Hossain Z, Kasinathan D, Rosner H, Geibel C and Gegenwart P 2008 *Phys. Rev. B* **78** 052502.
[18] Ren Z, Zhu Z, Jiang S, Xu X, Tao Q, Wang C, Feng C, Cao G H and Xu Z A 2008 *Phys. Rev. B* **78** 052501

[19] Miclea C F, Nicklas M, Jeevan H S, Kasinathan D, Hossain Z, Rosner H, Gegenwart P, Geibel C and Steglich F 2009 *Phys. Rev. B* **79** 212509
[20] Ren Z, Tao Q, Jiang S, Feng C, Wang C, Dai J, Cao G and Xu Z 2009 *Phys. Rev.Lett.* **102** 137002
[21] Jiao W H, Tao Q, Bao J K, Sun Y L, Feng C M, Xu Z A, Nowik I, Felner I and Cao G H 2011 *Europhys. Lett.* **95** 67007
[22] Jiang S, Xing H, Xuan G, Ren Z, Wang C, Xu Z A and Cao G 2009 *Phys. Rev. B* **80** 184514
[23] Paramanik U B, Das D, Prasad R and Hossain Z 2013 *J. Phys.: Condens. Matter* **25** 265701
[24] Jeevan H S, Hossain Z, Kasinathan D, Rosner H, Geibel C and Gegenwart P 2008 *Phys. Rev. B* **78** 092406
[25] Xiao Y, Su Y, Schmidt W, Schmalzl K, Kumar C M N, Price S, Chatterji T, Mittal R, Chang L J, Nandi S, Kumar N, Dhar S K, Thamizhavel A and Brueckel Th 2010 *Phys. Rev. B* **81** 220406(R)
[26] Maiwald J, Mazin I I and Gegenwart P 2018 *Phys. Rev. X* **8** 011011
[27] Jiang S, Luo Y K, Ren Z, Zhu Z W, Wang C, Xu X F, Tao Q, Cao G H and Xu Z A 2009 *New J. Phys.* **11** 025007
[28] Chuang M, Allan M P, Lee J, Xie Y, Ni N, Budko S L, Boebinger G S Canfield P C and Davis J C 2010 *Science* **327** 181
[29] Li S, Wilson S D, Mandrus D, Zhao B, Onose Y, Tokura Y and Dai P C 2005 *Phys. Rev. B* **71** 054505
[30] Lavrov A N, Kang H J, Kurita Y, Suzuki T, Komiya S, Lynn J W, Lee S H, Dai P C and Ando Y 2004 *Phys. Rev. Lett.* **92** 227003
[31] Perna P, Maccariello D, Ajejas F, Guerrero R, Mechin L, Flament S, Santamaria J, Miranda R and Camarero J 2017 *Advanced Functional Materials* **27** 1700664
[32] Man H R, Lu X Y, Chen J S, Zhang R, Zhang W L, Luo H Q, Kulda J, Ivanov A, Keller T, Morosan E, Si Q M and Dai P C 2015 *Phys. Rev. B* **92** 134521
[33] Yamada H and Takada S 1973 *J. Phys. Soc. Jpn.* **34** 51
[34] Xiao Y G, Su Y, Nandi S, Price S, Schmitz B, Kumar C M N, Mittal R, Chatterji T, Kumar N, Dhar S K, Thamizhavel A and Brückel Th 2012 *Phys. Rev. B* **85** 094504
[35] Nigam A K, Roy S B and Chaddah P 1999 *Phys. Rev. B* **60** 3002
[36] Radha S, Roy S B and Nigam A K 2000 *J. Appl. Phys.* **87** 6803
[37] Pippard A B 1989 *Magnetoresistance in Metals* (Cambridge: Cambridge University Press)